

PROCESSING AND PRODUCTS

Use of image analysis to identify woody breast characteristics in 8-week-old broiler carcasses

Juan P. Caldas-Cueva,^{*} A. Mauromoustakos,[†] X. Sun [‡] and Casey M. Owens ^{*,1}

^{*}Department of Poultry Science, University of Arkansas, Fayetteville, AR 72701, USA; [†]Agricultural Statistics Laboratory, University of Arkansas, Fayetteville, AR 72701, USA; and [‡]School of Biological Science and Food Engineering, Chuzhou University, Anhui 239000, China

ABSTRACT Woody breast (WB) condition causes significant economic losses to the global poultry industry, and the lack of an objective and fast tool to identify this myopathy is a contributing factor. The aim of this study was to determine if there are broiler carcass conformation changes that can be used to identify WB characteristics using image analysis. Images of 8-wk-old male broiler carcasses ($n = 544$) of high breast-yielding strains were captured before evisceration, which were processed and analyzed using ImageJ software. Measurements were as follows: M0, breast length; M1, breast width in the cranial region; M2, one-fifth of the breast length starting at the tip of keel; M3, breast width at the end of M2; M4, angle formed at the tip of keel and extending to outer points of M3; M5, area of the triangle formed by M3 and lines generated by M4; M6, area of the breast above M3; and M7, M6 minus M5. Ratios of these measurements were also considered. Whole breast fillets were scored for WB severity based on tactile assessment and compression

analysis to correlate them. Spearman's correlation coefficient (r_s) between WB scores and compression force was highly significant ($r_s = 0.83$, $P < 0.01$). Measurements M4 and M3 as well as ratios M9 (M3/M2) and M11 (M1/M0) had the highest correlation to the WB score ($r_s \geq 0.70$; $P < 0.01$) and compression force ($r_s \geq 0.64$; $P < 0.01$). The best validated model (generalized [Gen.] $R^2 = 0.60$) to predict WB included M1, M2, and M3. Using this model, 84% of broiler carcasses were correctly classified as WB or normal with a sensitivity of 82% to detect affected samples. Alternatively, M4 and M6 as well as ratios M9 and M11 could be considered as predictors in different models (Gen. $R^2 \geq 0.56$). The same predictors were significant to estimate compression force (Gen. $R^2 \geq 0.49$). These data support the use of image analysis to predict WB condition in broiler carcasses. The potential integration of these image measurements into commercial in-line vision grading systems would allow processors to sort broiler carcasses by WB severity.

Key words: woody breast, image analysis, processing, carcass grading, meat quality

2021 Poultry Science 100:100890
<https://doi.org/10.1016/j.psj.2020.12.003>

INTRODUCTION

An increasing and challenging meat quality problem in the global poultry industry is known as woody breast (WB) condition, a myopathy that can affect the consumer acceptance and generate important economic losses (Sihvo et al., 2014; Kuttappan et al., 2016; Caldas-Cueva and Owens, 2020). The WB defect is characterized by swollen and pale sections with significant

hardness in the raw chicken fillets (Sihvo et al., 2014; Mudalal et al., 2015). This myopathy exhibits histological signs of muscle fiber degeneration, lipidosis, and fibrosis that derive in chicken meat with higher levels of fat, collagen, and water and, thus, lower levels of protein and ash (Soglia et al., 2016; Wold et al., 2017; Velleman et al., 2018; Baldi et al., 2019), which negatively affects functional properties such as water-holding capacity and modifies texture attributes that result in downgrades and even condemnations (Hanning et al., 2018; Petracci et al., 2019). Objective and subjective methods have been applied to identify and characterize the WB anomaly in broiler breast fillets such as tactile evaluation for degree of hardness, instrumental texture analyses (Mudalal et al., 2015; Chatterjee et al., 2016; Tijare et al., 2016; Sun et al.,

© 2020 The Authors. Published by Elsevier Inc. on behalf of Poultry Science Association Inc. This is an open access article under the CC BY-NC-ND license (<http://creativecommons.org/licenses/by-nc-nd/4.0/>).

Received May 6, 2020.

Accepted December 1, 2020.

¹Corresponding author: cmowens@uark.edu

2018), and other detailed assessments such as metabolomics analysis and detection of differentially expressed genes (Abasht et al., 2016; Zambonelli et al., 2016).

Although scientists are trying to solve or reduce the WB incidence, the contemporary poultry industry demands objective, reliable, fast, nondestructive, and noncontact in-line methods such as image analysis to accurately identify or predict WB characteristics owing to its negative impact on broiler meat quality and yield. Image analysis supplies a useful tool for measuring the structure of foods, and one of its applications in the food industry is to control robotics for harvesting and sorting (Russ, 2015). The use of image analysis in the poultry industry is not a novel approach. Over the past decades, studies based on computer processing of images have been applied in the poultry industry to offer promising alternatives to carry out repetitive and tedious activities such as broiler carcass inspection and grading (Park and Chen, 1994; Chao et al., 2002; Martel and Paris, 2007; Barbin et al., 2016). Advanced methods have been evaluated to detect WB myopathy at a breast fillet level, such as the fusion of optical coherence tomography and hyperspectral imaging (Yoon et al., 2016), computer vision system, and near-infrared spectroscopy (Wold et al., 2017; Geronimo et al., 2019). However, early WB detection in poultry-processing plants would be needed to anticipate potential problems caused by WB defect on further processing operations such as deboning and portioning (Hanning et al., 2018). The prediction of WB condition would allow processors to identify and sort broiler carcasses by WB category. Processing plants would have the opportunity to work differentially with affected broiler carcasses and develop profitable applications of WB meat in further processed products such as chicken patties and deli loaves (Caldas-Cueva et al., 2020, 2021). In addition, processors would provide large-scale information upstream to live production (i.e., incidence rates or other valuable information to monitor factors associated with WB development) and downstream to further processing lines. Therefore, the objective of this study was to determine if there are conformational features that can be used to identify WB characteristics in commercial broiler carcasses using image analysis.

MATERIALS AND METHODS

Processing of Broiler

Male broiler carcasses ($n = 544$) from a commercial strain (high breast-yielding), aged 8 wk, were studied. All broilers were processed in 2 different trials at the University of Arkansas Poultry Processing Pilot Plant as per commercial-based practices (Mehaffey et al., 2006). Broilers were shackled, electrically stunned (11 V, 11 mA, 10 s), manually cut, bled out (1.5 min), scalded (54°C, 2 min), picked in-line using defeathering equipment, manually eviscerated, and rinsed. After evisceration, carcasses were prechilled at 12°C for 15 min and chilled for 90 min at 1°C in immersion tanks. Broiler

carcasses were manually agitated at consistent intervals throughout the chilling process. Carcasses without giblets (**WOG**) were then removed, packed in ice, and stored in a walk-in cooler at 4°C until the deboning time at 3 h postmortem. All animal handling procedures complied with the Institutional Animal Care and Use Committee at the University of Arkansas, Fayetteville.

Image Collection

Images of broiler carcasses were captured before evisceration against a black background to have a sharp outline of the carcass conformation under consistent ambient lighting conditions (light source: light-emitting diodes, 5,000 k). The orientation of the carcass hanging vertically down was such that its breast section was facing the camera, as shown in Figure 1. In addition, a ruler was vertically aligned on the background to set the scale during image processing and analysis. A Canon EOS 60D digital single-lens reflex (**DSLR**) camera (Canon USA Inc., Lake Success, NY) was used to capture images. The camera was placed centrally in front of the carcass at 1.32 m of distance from the camera lens to the shackle line. For image collection, the camera was set to $2,592 \times 1,728$ pixels and a spatial resolution of 72 ppi. Images were captured with an exposure time of 1/60 s, ISO of 1,600, and opening f/5 with a format of the JPG image file.

Deboning and Tactile Evaluation

Carcasses were manually deboned by severing the humeral–scapular joint and pulling firmly downward on the wings at 3 h postmortem after chilling. The deboned breast fillets (pectoralis major) were successively scored for the degree of hardness by tactile evaluation (Tijare et al., 2016). The WB categorization considered in tactile evaluation was the following: 0.0 or 0.5 as normal–NOR or unaffected fillets of flexible consistency throughout; 1.0 or 1.5 as mild–MIL or partially affected fillets of hard consistency mainly in the cranial region with some flexibility in the middle to caudal region, and 2.0, 2.5, or 3.0 for moderate to severe cases of WB myopathy–SEV or affected fillets of very hard and firm consistency throughout with limited or nonexistent flexibility in the middle to caudal region. After scoring, breast fillets were stored for a brief period in a cooler (4°C) until instrumental texture analysis, which was carried out to validate subjective tactile scores at approximately 6 h postmortem.

Compression Force Analysis

Compression force (**CF**) analysis was carried out as per the method described by Sun et al. (2018) with some modifications. In brief, this instrumental texture measurement was determined in quadruplicate at predetermined locations in the cranial region of each intact breast fillet using a texture analyzer (model TA.XT Plus; Texture Technologies Corp., Scarsdale, NY). Fillet

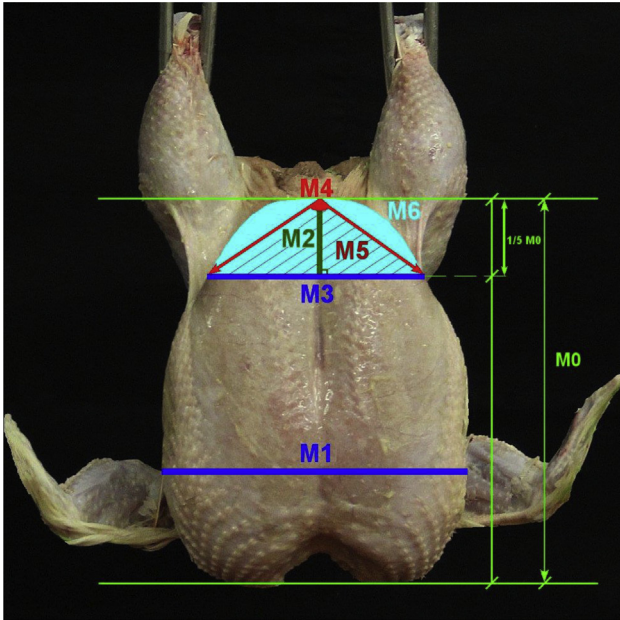


Figure 1. Structural information from broiler carcass images. Parameters for carcass conformation: M0, breast length; M1, breast width in the cranial region; M2, a vertical line from the tip of keel to one-fifth of breast length; M3, breast width at the end of M2; M4, angle formed at the tip of keel and extending to outer points of M3; M5, area of the triangle formed by M3 and lines generated by M4; M6, area of the breast above M3.

samples were compressed to 20% of their original height using a 6-mm-diameter flat probe with the following conditions: a pretest speed of 10.0 mm/s, a test speed of 5.0 mm/s, a post-test speed of 10.0 mm/s, a load cell capacity of 5 kg, and a trigger force of 5 g.

Image Processing and Analysis

After collection, two-dimensional and frontal images were processed using ImageJ software (National Institutes of Health, Bethesda, MD). Some image processing functions were used such as vertical rotation and sharpening. The region of interest was focused on the breast from which various parameters for carcass conformation were considered, as described in Table 1 and shown in Figure 1. In detail, fixed horizontal reference lines were initially drawn tangential to the tip of the keel region and the bottom end of the right side of the cranial region to extract the carcass measurements. Thus, M0 was the breast length or the vertical distance between reference lines described previously; M1 was the breast width in the cranial region (horizontal line in the widest section); M2 was the vertical line from the tip of keel to one-fifth of breast length; M3 was the breast width at the end of M2; M4 was the angle formed at the tip of keel and extending to outer points of M3; M5 was the area of the triangle formed by M3 and lines generated by M4; M6 was the area of the breast above the M3 line, and M7 was the difference of following areas: M6 minus M5. In addition, 4 ratios (ratio of M3 to M1 [M8], ratio of M3 to M2 [M9], ratio of M7 to M5 [M10], and ratio of M1 to M0 [M11]) were considered in this study.

Table 1. Structural information from broiler carcass images.

Measurement	Description
M0	Breast length
M1	Breast width in the cranial region
M2	A vertical line from the tip of keel to one-fifth of breast length (right side)
M3	Breast width at the end of M2 segment
M4	Angle formed at the tip of keel and extending to outer points of M3
M5	Area of the triangle formed by M3 and lines generated by M4
M6	Area of the breast section formed above M3 segment
M7	M6 – M5 (difference of areas M6 and M5)
M8	The ratio of M3 to M1
M9	The ratio of M3 to M2
M10	The ratio of M7 to M5
M11	The ratio of M1 to M0

Statistical Analysis

Spearman's correlation coefficients (r_s) were investigated for WB severity scores, CF values, and image measurements. For comparison purposes, the WB classes were recategorized into 2 groups to create a binary response data of WB condition status (no = unaffected or mildly affected fillets [WB scores from 0.0 to 1.5] and yes = moderately or severely affected fillets [WB scores from 2.0 to 3.0]). Least-squares fit was carried out for description of WB categories (NOR, MIL, and SEV) and binary response (yes/no) based on image measurements from broiler carcasses and instrumental texture analysis in their corresponding breast fillets. The main effect of WB category or WB status was fitted as a fixed effect. When the main effect was significant, means were separated using Tukey's honestly significant difference test and the Student t test at $P < 0.05$ for WB categories and binary response, respectively. A stratified random split was used to divide the data into 2 sets of 70 and 30% for training and validation, respectively. The generalized regression platform was initially used to evaluate and select the best subsets of carcass measurements or predictors to be incorporated into feasible models for predicting WB condition. Subsequently, the ordinal logistic regression platform was used to develop and assess prediction models using the selected subsets of predictors for the classification of broiler carcasses into three WB categories. In parallel, binary logistic regression analysis was carried out to build and evaluate prediction models using the same selected subsets of predictors with a binomial distribution for WB condition status. Four statistical outputs were used to assess the classification performance of prediction models: the overall misclassification rate (MR) or proportion of wrong predictions or one minus the overall accuracy of the model, the true-positive rate (TPR) or sensitivity that was estimated as the ratio of the number of correctly classified samples as positive to the total number of positives or samples with moderate or severe levels of WB condition, false-positive rate (FPR) or one minus specificity that was estimated as the ratio of the number of incorrectly classified samples as positive to

the total number of negatives, and area under the receiver operating characteristic curve (**AUC**). In addition, generalized (**Gen.**) R^2 , root mean square error (**RMSE**), and mean absolute deviation (**MAD**), and Akaike Information Criterion (**AIC**) were also evaluated. The generalized regression platform was also performed to develop and assess prediction models using the same selected subsets of predictors with a log-normal distribution for CF. The adaptive elastic net was selected as the estimation method with the validation column for authentication process. Statistical analysis was achieved using JMP software, version 14.1.0 (SAS Institute Inc., Cary, NC).

RESULTS AND DISCUSSION

Image Measurements and CF

The results from this study showed that image measurements from broiler carcasses and the CF of their corresponding deboned breast fillets were significantly different among WB categories ($P < 0.01$) (Table 2). The images shown in Figure 2 illustrate the differences in carcass dimensions among the three WB categories. Broiler carcasses that yielded breast fillets with SEV levels of WB condition showed greater breast width at cranial (M1) and caudal (M3) regions ($P < 0.05$) as well as greater angles at the tip of keel (M4) and breast areas in the caudal section (M5, M6, and M7) ($P < 0.05$) in comparison with NOR samples. However, the breast length (M0) and the vertical line from the tip of keel to one-fifth of breast length (M2) were shorter for broiler carcasses more severely affected by WB condition than for NOR specimens ($P < 0.05$). With exception to M0 and M2, intermediate dimensions were achieved for MIL samples ($P < 0.05$). There have been no reports

of morphometric changes in broiler carcasses exhibiting WB characteristics; nevertheless, there are some studies that report that the occurrence and severity of WB and white striping myopathies are associated with thicker and heavier (Mudalal et al., 2015; Petracci et al., 2019) and wider (Zambonelli et al., 2016) breast fillets than with unaffected samples. Indeed, it has been corroborated in this study that whole breast fillet weights were different among WB categories ($P < 0.01$). Broiler live and carcass WOG weights were also different among the WB groups ($P < 0.01$). Broiler carcasses that yielded MIL and SEV breast fillets were heavier than those that yielded NOR fillets, whereas NOR and MIL breast fillets were lighter than SEV fillets ($P < 0.05$). On the other hand, when analyzing the description of binary response (WB condition status: yes or no), all image measurements and CF values were significantly different between WB status responses ($P < 0.01$). Similarly, live, carcass WOG, and fillet weights were significantly different from each other (WB yes > WB no; $P < 0.05$).

With respect to the CF, breast fillets for broilers more severely affected by WB condition presented the greatest CF ($P < 0.05$), whereas NOR samples had the lowest CF ($P < 0.05$). Intermediate CF values were achieved for MIL samples that were lower than for SEV samples, but greater than for NOR samples ($P < 0.05$). The CF results of this research are similar to recent publications that report higher CF values in breast fillets with SEV levels of WB condition than with unaffected samples (Soglia et al., 2017; Dalggaard et al., 2018; Sun et al., 2018; Baldi et al., 2019; Caldas-Cueva et al., 2020, 2021). On the other hand, relationships between image measurements from broiler carcasses, WB fillet scores, and CF values were investigated. The positive correlation between WB severity scores and CF was highly significant ($r_s = 0.83$, $P < 0.01$). M9 (M3/M2), M4 (angle

Table 2. Description of woody breast (WB) categories and binary response (WB status) based on image measurements from broiler carcasses and instrumental texture analysis in their corresponding breast fillets.

Variable	Woody breast category ¹			Woody breast status ²	
	NOR	MIL	SEV	No	Yes
Live weight (g)	4,036 ± 26 ^b	4,168 ± 22 ^a	4,217 ± 24 ^a	4,108 ± 17 ^b	4,217 ± 24 ^a
Carcass (WOG) ³ weight (g)	3,199 ± 21 ^c	3,325 ± 19 ^b	3,391 ± 20 ^a	3,268 ± 14 ^b	3,391 ± 20 ^a
Fillet weight (g)	934 ± 8 ^c	1,026 ± 7 ^b	1,114 ± 8 ^a	984 ± 6 ^b	1,114 ± 8 ^a
Compression force (N)	4.39 ± 0.11 ^c	7.18 ± 0.18 ^b	11.80 ± 0.29 ^a	5.91 ± 0.13 ^b	11.80 ± 0.29 ^a
M0 (cm)	26.82 ± 0.09 ^a	26.69 ± 0.07 ^a	26.25 ± 0.07 ^b	26.75 ± 0.06 ^a	26.25 ± 0.07 ^b
M1 (cm)	18.33 ± 0.05 ^c	18.97 ± 0.05 ^b	19.50 ± 0.05 ^a	18.68 ± 0.04 ^b	19.50 ± 0.05 ^a
M2 (cm)	5.36 ± 0.02 ^a	5.34 ± 0.01 ^a	5.25 ± 0.01 ^b	5.35 ± 0.01 ^a	5.25 ± 0.01 ^b
M3 (cm)	11.67 ± 0.06 ^c	12.51 ± 0.07 ^b	13.70 ± 0.07 ^a	12.13 ± 0.05 ^b	13.70 ± 0.07 ^a
M4 (°)	94.34 ± 0.34 ^c	98.36 ± 0.35 ^b	104.44 ± 0.31 ^a	96.54 ± 0.27 ^b	104.44 ± 0.31 ^a
M5 (cm ²)	31.31 ± 0.20 ^c	33.39 ± 0.22 ^b	35.96 ± 0.21 ^a	32.44 ± 0.16 ^b	35.96 ± 0.21 ^a
M6 (cm ²)	40.49 ± 0.32 ^c	43.93 ± 0.35 ^b	49.23 ± 0.38 ^a	42.37 ± 0.26 ^b	49.23 ± 0.38 ^a
M7 (cm ²)	9.17 ± 0.18 ^c	10.54 ± 0.19 ^b	13.26 ± 0.21 ^a	9.92 ± 0.14 ^b	13.26 ± 0.21 ^a
M8	0.64 ± 0.00 ^c	0.66 ± 0.00 ^b	0.70 ± 0.00 ^a	0.65 ± 0.00 ^b	0.70 ± 0.00 ^a
M9	2.18 ± 0.01 ^c	2.35 ± 0.01 ^b	2.61 ± 0.01 ^a	2.27 ± 0.01 ^b	2.61 ± 0.01 ^a
M10	0.29 ± 0.01 ^c	0.32 ± 0.01 ^b	0.37 ± 0.00 ^a	0.30 ± 0.00 ^b	0.37 ± 0.00 ^a
M11	0.68 ± 0.00 ^c	0.71 ± 0.00 ^b	0.74 ± 0.00 ^a	0.70 ± 0.00 ^b	0.74 ± 0.00 ^a

^{a-c}Means ± SEM with no common superscripts within a row are significantly different ($P < 0.05$).

M0 to M11: Broiler carcass dimensions described in Table 1.

¹NOR: normal breast fillets (n = 154); MIL: mild WB fillets (n = 185); SEV: moderate or severe WB fillets (n = 205).

²No: normal or mildly affected fillets by WB condition (n = 339); Yes: fillets moderately or severely affected by WB condition (n = 205).

³WOG: carcass without giblets.

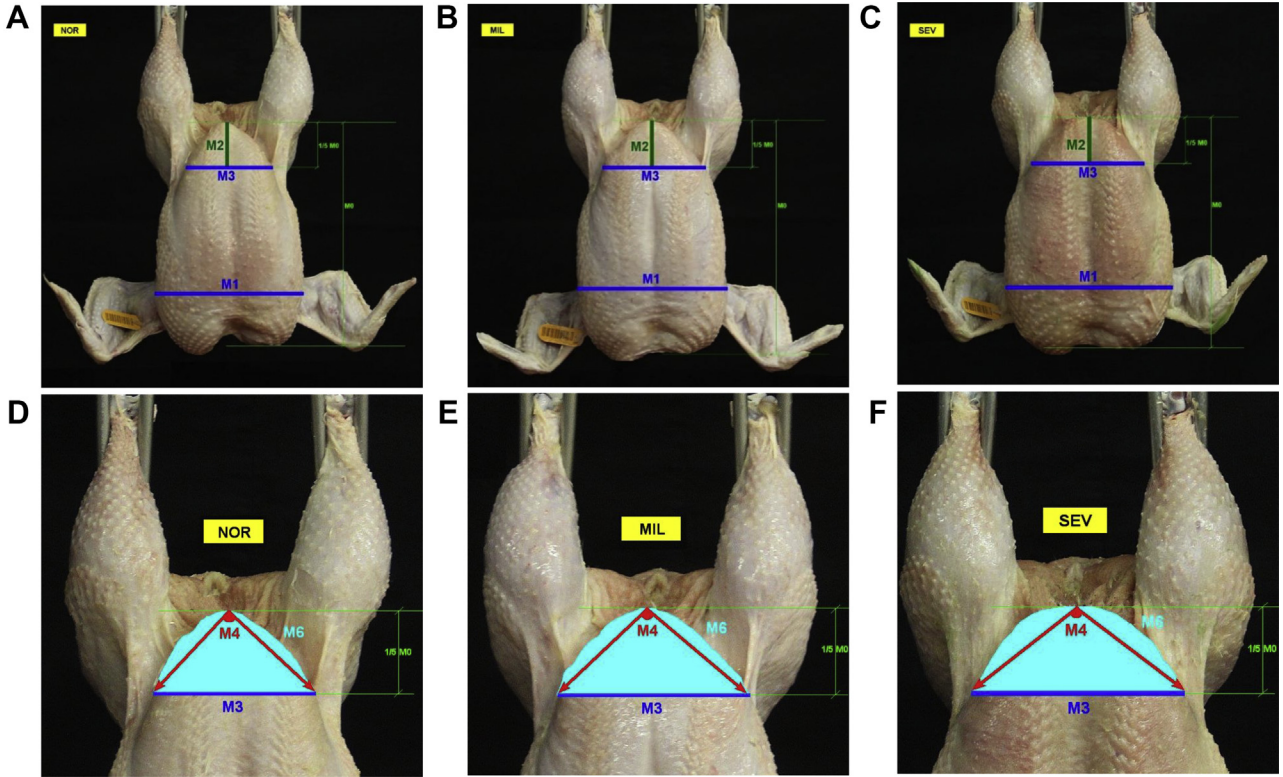


Figure 2. Image measurements that can be potentially included in prediction models to identify woody breast (WB) condition in commercial broiler carcasses. (A, D) M1, M2, M3, M4, and M6 measurements of broiler carcass that yielded unaffected or NOR fillets. (B, E) M1, M2, M3, M4, and M6 measurements of broiler carcass that yielded fillets partially affected by WB (MIL). (C, F) M1, M2, M3, M4, and M6 measurements of broiler carcass that yielded fillets moderately or severely affected by WB (SEV).

at keel), M3 (caudal breast width), and M11 ($M1/M0$) had the highest correlation to WB scores ($r_s \geq 0.70$; $P < 0.01$) and CF ($r_s \geq 0.64$; $P < 0.01$), followed by measurements M6, M1, M5, M7, M8, and M10, respectively, whereas M2 and M0, showing the lowest coefficients, were inversely correlated with WB scores ($r_s = -0.22$, $P < 0.01$) and CF ($r_s = -0.18$, $P < 0.01$) (Figure 3).

Modeling of WB Prediction in Broiler Carcasses Using Image Measurements

Images ($n = 544$) collected from commercial high breast-yielding broiler carcasses were used to develop models for predicting WB condition. Eight image measurements (M0 through M7) and four ratios (M8 [$M3/M1$], M9 [$M3/M2$], M10 [$M7/M5$], and M11 [$M1/M0$]) were considered in statistical analysis, from which 4 parameters were used to evaluate the quality of the prediction model (MR [%], TPR [%] or sensitivity, FPR [%] and AUC) in addition to the Gen. R^2 , RMSE, and MAD outputs. From the total number of images, 381 were used for model development (training; 70% of data), and 163 were used for validation (30% of data). These measurements were initially used to predict three WB categories: normal, NOR (scores: 0.0–0.5); mild, MIL (scores: 1–1.5); and severe, SEV (scores: 2–3) using an ordinal logistic regression analysis from which the performance of the simplest and most suitable prediction

model is shown in the Table 3. Using this model and regardless of the data set, less than 1% of NOR carcasses were misclassified as SEV samples, whereas more than 35% of NOR carcasses were misclassified as MIL samples. For the SEV category, there were less than 2% misclassified into the NOR group and more than 23% misclassified into the MIL category (Table 3). The overall accuracy of this ordinal logistic regression model with the best subset of predictors (M1, M2, and M3) was lower (MR > 35%) than that for the binary logistic regression model (MR < 20%). This difference in classification accuracy could be explained by the fact that MIL samples were considerably misclassified into NOR and SEV categories, which could be expected as these samples are intermediate in structural features along with meat quality characteristics when compared with the other WB categories. Thus, the binary response (no: WB scores ≤ 1.5 and yes: WB scores ≥ 2.0) using a binary logistic regression analysis was considered to evaluate and select suitable prediction models for WB condition.

Table 4 presents the most satisfactory prediction models for WB condition status based on their predictive performance results (MR $\leq 18.37\%$, TPR $\geq 71.53\%$, FPR $\leq 13.08\%$, AUC ≥ 0.89 , Gen. $R^2 \geq 0.56$, RMSE = 0.36, and MAD ≤ 0.26). These models included 6 subsets of predictors ($P < 0.01$) as follows: 3 models using image measurements (M1, M2, and M3 [model 1], M1, M2, and M4 [model 2], and M1, M2,

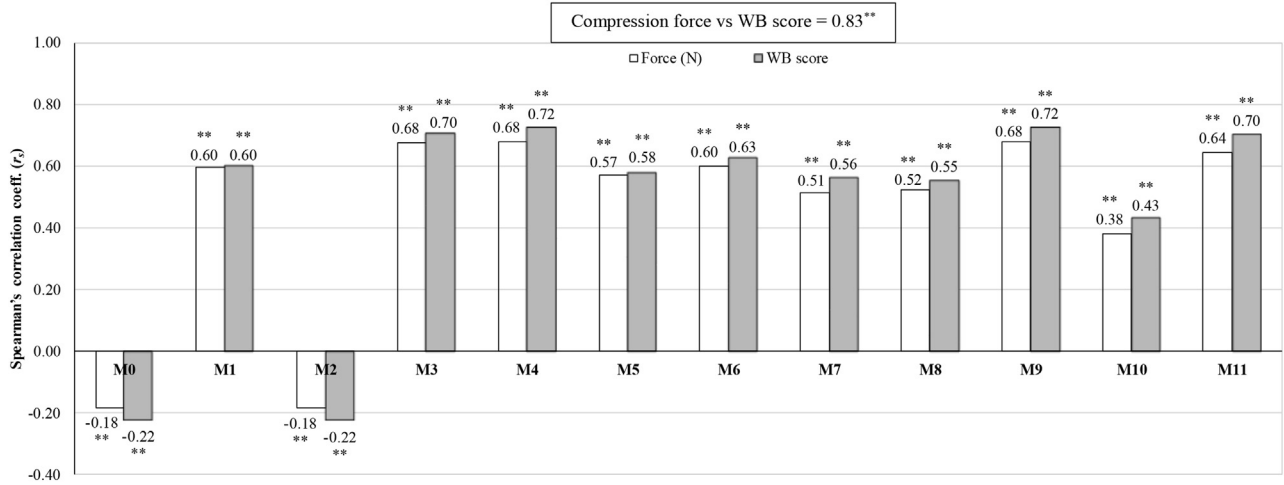


Figure 3. Correlations of image measurements with WB tactile scores and compression force. **Spearman's correlation coefficient (r_s) was significant ($P < 0.01$). Abbreviation: WB, woody breast.

and M6 [model 3]), one model using ratios (M9 and M11 [model 4]), and 2 models using a mixture of an image measurement and a ratio (M1 and M9 [model 5] and M3 and M11 [model 6]). Regardless of the model, the proportion of wrong predictions was less than 19%, the proportion of broiler carcasses that were correctly identified as affected samples with WB condition was higher than 71%, and the proportion of broiler carcasses that were incorrectly classified as affected samples with WB condition was lower than 14%. In addition, the ability of the models to distinguish the 2 levels of the binary response was between good (AUC ~ 0.89) and excellent (AUC ~ 0.90). Among these models, model 1 had the lowest MR (17.06%), followed by models 2, 6, 5, 4, and 3, respectively. Models 1 and 2 showed the highest levels of sensitivity (TPR $\geq 75\%$), whereas models 4 and 5 had the lowest FPR (11.81%). When validating the models, the results of Gen. R^2 (≥ 0.57), RMSE (≤ 0.35), MAD (≤ 0.25), MR ($\leq 19.02\%$), and AUC (≥ 0.90) were

Table 3. Classification of 8-week-old broiler carcasses into WB categories using M1, M2, and M3 measurements in an ordinal logistic regression model.

Fit details ¹				Predicted count ²			
Gen. R^2	RMSE	MAD	MR (%)	Actual	NOR	MIL	SEV
Training							
0.62	0.50	0.43	35.17	NOR	69	38	1
				MIL	28	71	31
				SEV	2	34	107
Validation							
0.51	0.53	0.46	40.49	NOR	27	19	0
				MIL	14	27	14
				SEV	1	18	43

Abbreviation: MAD, mean absolute deviation; MR, misclassification rate; RMSE, root mean square error; WB, woody breast.

¹A stratified random split was used to divide the data into 2 sets of training ($n = 381$) and validation ($n = 163$).

²NOR: broiler carcasses that yielded unaffected fillets; MIL: broiler carcasses that yielded fillets partially affected by WB; SEV: broiler carcasses that yielded fillets moderately or severely affected by WB.

comparable, whereas the TPR ($\geq 78.69\%$) and FPR ($\leq 17.65\%$) values increased on average 6.99 and 3.22%, respectively.

From these 6 models, the simplest validated prediction model for WB condition included M1, M2, and M3 measurements or a mixture of the M1 measurement and M9 ratio ($P < 0.01$); other potential predictors (M4, M6, and M11) require more complex procedures to determine measurements. However, poultry processors would improve and define the best model as per the capability of commercial in-line vision graders. There are vision grading systems to inspect and classify broiler carcasses, which basically consist of a digital camera, appropriate lighting, and sophisticated recognition software. These advanced systems can detect multiple poultry carcass defects such as missing parts, holes in certain parts, and abnormal skin conditions that downgrade the poultry meat quality (Martel and Paris, 2007). In terms of shape and dimensions, Chao et al. (2010) reported that multispectral image processing, which mechanically identifies the region of interest on broiler carcass images, may be incorporated into commercial high-speed inspection systems to control the their quality condition. In another study, the imaging technique was applied to estimate the live weight of broilers using their body surface-area pixels via a linear equation (Mollah et al., 2010). There have been no reports of using such systems to detect WB in broiler carcasses.

Table 4 also shows the odds ratios corresponding to each binary logistic model. Odds ratios represent the proportional change in the odds of obtaining an affected sample with WB condition compared with the unaffected sample for each unit change in the predictor (M1, M2, and so on). For example, analyzing the odds ratios for model 1, the odds of observing an affected sample with WB condition were 3.25 times higher with 1-cm increase in the breast width at the cranial region (M1), and the odds were 3.17 times higher with 1-cm increase

Table 4. Binary logistic regression models to predict woody breast (WB) condition in 8-week-old broiler carcasses using image measurements.

Prediction model ¹	Data set ²	Fit details							Parameter estimates and odds ratio (OR)				
		Gen. R ²	RMSE	MAD	MR (%)	TPR (%)	FPR (%)	AUC	Parameter	Estimate	Std. Error	Pr > χ^2	OR
Model 1	Training	0.57	0.36	0.25	17.06	75.00	12.24	0.89	M1	1.18	0.28	<0.0001	3.25
	Validation	0.60	0.34	0.24	15.95	81.97	14.71	0.91	M2	-4.81	0.91	<0.0001	8.16×10^{-3}
									M3	1.15	0.18	<0.0001	3.17
Model 2	Training	0.57	0.36	0.25	17.32	75.69	13.08	0.90	M1	1.19	0.28	<0.0001	3.27
	Validation	0.61	0.34	0.23	16.56	81.97	15.69	0.91	M2	-2.26	1.01	0.0245	0.10
									M4	0.27	0.04	<0.0001	1.31
Model 3	Training	0.57	0.36	0.25	18.37	71.53	12.24	0.89	M1	1.30	0.27	<0.0001	3.66
	Validation	0.59	0.35	0.24	19.02	78.69	17.65	0.91	M2	-6.29	0.92	<0.0001	1.86×10^{-3}
									M6	0.22	0.04	<0.0001	1.25
Model 4	Training	0.56	0.36	0.26	17.85	72.22	11.81	0.89	M9	6.11	0.97	<0.0001	4.48×10^2
	Validation	0.57	0.35	0.25	17.18	78.69	14.71	0.90	M11	23.76	6.49	0.0003	2.08×10^{10}
Model 5	Training	0.56	0.36	0.25	17.59	72.92	11.81	0.89	M1	0.87	0.22	<0.0001	2.38
	Validation	0.58	0.35	0.24	17.18	80.33	15.69	0.90	M9	7.18	0.86	<0.0001	1.31×10^3
Model 6	Training	0.57	0.36	0.25	17.59	74.31	12.66	0.90	M3	1.12	0.17	<0.0001	3.06
	Validation	0.60	0.34	0.24	15.95	81.97	14.71	0.91	M11	33.62	5.90	<0.0001	3.99×10^{14}

M1, M2, ...Mn are the independent predictor variables (image measurements), α is the intercept, and $\beta_1, \beta_2, \dots, \beta_n$ are the regression coefficients. AUC, area under the receiver operating characteristic curve; FPR, false-positive rate; MAD, mean absolute deviation; MR: misclassification rate; RMSE: root mean square error; TPR, true-positive rate (sensitivity).

¹Model 1 = $\text{Logit}(p) = \alpha + \beta_1 M1 + \beta_2 M2 + \beta_3 M3$. Model 2 = $\text{Logit}(p) = \alpha + \beta_1 M1 + \beta_2 M2 + \beta_3 M4$. Model 3 = $\text{Logit}(p) = \alpha + \beta_1 M1 + \beta_2 M2 + \beta_3 M6$. Model 4 = $\text{Logit}(p) = \alpha + \beta_1 M9 + \beta_2 M11$. Model 5 = $\text{Logit}(p) = \alpha + \beta_1 M1 + \beta_2 M9$. Model 6 = $\text{Logit}(p) = \alpha + \beta_1 M3 + \beta_2 M11$.

²A stratified random split was used to divide the data into 2 sets of training (n = 381) and validation (n = 163).

in the caudal region (M3) of broiler carcasses. These results could be related to the findings reported by Zambonelli et al. (2016), who found that broiler breast fillets affected by WB disorder were significantly wider than normal fillets ($P < 0.01$), which might explain to some extent the differences in the conformational features between affected and normal broiler carcasses. In addition, researchers have reported consistently that breast fillets affected by WB are thicker at cranial, medial, and caudal regions of the breast than normal broiler breast dimensions (Mudalal et al., 2015; Zambonelli et al., 2016), which may also contribute to explain the differences in carcass conformation identified through image measurements. Sihvo et al. (2014) observed ridge-like bulges at the caudal end of breast fillets with WB anomaly; in fact, this feature has been suggested as a discriminant parameter to detect WB fillets (Mudalal et al., 2015). In contrast, the odds of observing an affected sample with WB condition became 99.18% smaller with 1-cm increase in the 20% of breast length (M2) of broiler carcasses. When analyzing the odds ratios for the other image measurements in model 2 (M4) and model 3 (M6), the odds of detecting an affected sample with WB myopathy increased by 30.66 and 24.53% with one-degree increase in the angle at keel tip (M4) and one square centimeter increase in the breast area at the caudal region (M6) of broiler carcasses, respectively.

The effectiveness of the prediction model for WB condition status was determined by introducing the average of M1, M2, and M3 measurements of both NOR samples and broiler carcasses that yielded breast fillets exhibiting SEV levels of WB condition in the prediction profiler of the nominal logistic platform. From this analysis, the probability of detection of WB condition in SEV samples was 77.42%, whereas using the average M1, M2, and M3

measurements of NOR or unaffected samples, the probability of detection of WB condition was drastically reduced to 11.65% (Table 6). These results demonstrate the precision and accuracy of the model predicting WB condition in broiler carcasses. Although there are no previous reports that have evaluated objective methods for WB prediction in broiler carcasses, there are some studies that applied advanced methods to detect WB myopathy at a breast fillet level such as the fusion of optical coherence tomography and hyperspectral imaging (Yoon et al., 2016), computer vision system, and near-infrared spectroscopy (Wold et al., 2017; Geronimo et al., 2019). Using a computer vision system, Geronimo et al. (2019) reported a 91.8% of accuracy to classify normal and chicken breast samples affected by WB anomaly by combining image analyses using a Support Vector Machine classification model. In this study, using the best validated model, a slightly lower accuracy (84.05%) was achieved; however, the use of 3 carcass dimensions (M1, M2, and M3) to potentially sort broiler carcasses by WB severity could be advantageous by anticipating quality defects that could occur in further processing operations such as portioning, deboning, and marination.

Estimation of CF in Deboned Breast Fillets

The objective of this section was to estimate the CF, an objective instrumental method to evaluate fillet hardness, using objective image measurements. Models from this analysis could provide a more objective method to classify fillets into WB categories. To maintain consistency in the study, the best subsets of variables for WB prediction in commercial broiler carcasses were considered in the statistical analysis to estimate the CF in their corresponding deboned breast fillets (M1,

Table 5. Generalized regression models to estimate compression force in deboned breast fillets from 8-wk-old broiler carcasses using image measurements.

Prediction model ¹	Fit details				Parameter estimates			
	Data set ²	Gen. R ²	-LogLikelihood	AICc	Parameter	Estimate	Standard error	Pr > χ^2
Model A	Training	0.53	881.59	1773.35	M1	0.240	0.027	<0.0001
	Validation	0.63	375.66	761.70	M2	-0.606	0.090	<0.0001
Model B					M3	0.149	0.019	<0.0001
	Training	0.52	883.51	1777.19	M1	0.246	0.027	<0.0001
	Validation	0.65	372.99	756.37	M2	-0.307	0.113	0.0067
Model C					M4	0.032	0.004	<0.0001
	Training	0.51	888.09	1786.33	M1	0.270	0.027	<0.0001
	Validation	0.61	380.77	771.92	M2	-0.806	0.086	<0.0001
Model D					M6	0.026	0.004	<0.0001
	Training	0.49	895.93	1799.96	M9	0.778	0.102	<0.0001
	Validation	0.59	385.53	779.32	M11	4.667	0.694	<0.0001
Model E	Training	0.52	883.15	1774.40	M1	0.203	0.023	<0.0001
	Validation	0.64	375.42	759.09	M9	0.945	0.076	<0.0001
Model F	Training	0.52	883.57	1775.25	M3	0.164	0.018	<0.0001
	Validation	0.63	377.06	762.38	M11	5.334	0.570	<0.0001

Model D: CF = $e^{(\alpha + \beta_1 M_9 + \beta_2 M_{11})}$. Model E: CF = $e^{(\alpha + \beta_1 M_1 + \beta_2 M_9)}$. Model F: CF = $e^{(\alpha + \beta_1 M_3 + \beta_2 M_{11})}$.
¹Compression force (CF): model A, CF = $e^{(\alpha + \beta_1 M_1 + \beta_2 M_2 + \beta_3 M_3)}$; model B, CF = $e^{(\alpha + \beta_1 M_1 + \beta_2 M_2 + \beta_3 M_4)}$; model C: CF = $e^{(\alpha + \beta_1 M_1 + \beta_2 M_2 + \beta_3 M_6)}$.

²A stratified random split was used to divide the data into 2 sets of training (n = 381) and validation (n = 163).

M2, and M3 [model A], M1, M2, and M4 [model B], and M1, M2, and M6 [model C], M9 and M11 [model D], M1 and M9 [model E], and M3 and M11 [model F]). Although a critical difference was not observed among these 6 models, model A showed the highest Gen. R² (0.53) and the lowest -LogLikelihood (881.59) and AICc (1773.35) values, whereas model D presented the lowest Gen. R² (0.49) and the highest -LogLikelihood (895.93) and AICc (1799.96) values. When validating the models, model B showed the highest Gen. R² (0.65) and the lowest -LogLikelihood (372.99) and AICc (756.37) values, whereas model D also presented the lowest Gen. R² (0.59) and the highest -LogLikelihood (385.53) and AICc (779.32) values. These results indicate that the most suitable prediction models were models A and B; however, similar to the results of WB prediction, the best and simplest validated prediction model for CF included M1, M2, and M3 measurements.

Table 5 also shows the parameter estimates for each generalized regression model. Parameter estimates are the change in the response (CF) associated with a

one-unit change of the predictor (M1, M2, and so on), holding all other predictors constant. For example, analyzing the parameter estimates for model A, holding all other predictors constant, 1-cm increase in the breast width at the cranial region (M1) led to 23.95% increase in CF; this increase was 14.86%, with 1-cm increase in the caudal region (M3) of broiler carcasses. On the contrary, 1-cm increase in the 20% of breast length (M2) of broiler carcasses led to 60.58% decrease in CF, holding all other predictors constant. Analyzing the parameter estimates for the other image measurements in model B (M4) and model C (M6), holding all other predictors constant, one-degree increase in the angle at keel tip (M4) and one square centimeter increase in the breast area at the caudal region (M6) of broiler carcasses led to 3.18 and 2.58% increase in CF, respectively.

Introducing the average of each image measurement of model A (M1, M2, and M3) of samples exhibiting severe levels of WB condition in the prediction profiler of the generalized regression platform, the estimated CF was 10.48 N, whereas using the average values of M1, M2,

Table 6. Prediction of woody breast (WB) condition and compression force in deboned breast fillets from 8-wk-old broiler carcasses using image measurements.

Broiler carcass ¹	Image measurement ² (cm)	Prediction ³					
		WB status ³		Most likely	Compression force (N) ⁴	95% CI	
		Probability (yes)	Probability (no)				
Normal samples	M1	18.68	11.65%	88.35%	No	6.42	6.18–6.67
	M2	5.35					
	M3	12.13					
WB samples	M1	19.50	77.42%	22.58%	Yes	10.48	10.00–10.98
	M2	5.25					
	M3	13.70					

¹Normal samples: broiler carcasses that yielded unaffected or mildly affected fillets; WB samples: broiler carcasses that yielded fillets moderately or severely affected by WB condition.

²Mean values of M1 (breast width in the cranial region), M2 (vertical line from the tip of keel to one-fifth of breast length), and M3 (breast width at the end of M2) measurements.

³Prediction regression for WB status (model 1): $\text{Logit}(p) = \alpha + \beta_1 M_1 + \beta_2 M_2 + \beta_3 M_3$.

⁴Prediction regression for compression force (model A): $\text{CF} = e^{(\alpha + \beta_1 M_1 + \beta_2 M_2 + \beta_3 M_3)}$.

and M3 for NOR or unaffected samples, the estimated CF was 6.42 N (Table 6). These estimated CF values were comparable with those measurements determined using the texture analyzer in the laboratory (Table 2). On the other hand, it was found that the estimated CF values were 5.48, 7.32, and 10.48 for NOR, MIL, and SEV categories, respectively, using their corresponding M1, M2, and M3 measurements. These estimated CF values were also comparable with those measurements determined using the texture analyzer in the laboratory (Table 2). Although objective methods such as hyperspectral imaging technique, that combines characteristics of spectroscopy and imaging techniques, has been used to predict broiler breast fillet tenderness (Jiang et al., 2018), it has not been found references of the use of objective morphometric changes in broiler carcasses to predict another objective measurement such as CF, which makes the proposed prediction model a unique method to estimate this important instrumental texture characteristic. Nevertheless, the application of these models based on a wide range of data by using multiple broiler strains and ages needs to be investigated to confirm that WB myopathy has some shape features that are visible at the carcass level independent of bird genetics and size.

In conclusion, the results from this study showed that there are conformational changes in the carcass breast region that could be used to identify WB characteristics in commercial broilers using image analysis. The CF of intact raw breast fillets, which was highly correlated to WB tactile scores, was the objective support to confirm the WB prediction using image measurements. The accuracy and precision of the application of this method using automated in-line computer vision systems might depend on several factors such as the adequate procedure of image acquisition, processing, and analysis using reliable software with the ability to locate, measure, and analyze the proposed broiler carcass measurements to detect this myopathy. The potential integration of these image measurements into commercial in-line vision grading systems would allow processors to identify and sort broiler carcasses by WB category in addition to providing large-scale information to the poultry industry. However, further studies are required to validate relationships when broilers from other ages, strains, and gender are included.

ACKNOWLEDGMENTS

This project was supported by the U.S. Poultry & Egg Association (Project F072). The authors are appreciative of Sara Landis (University of Arkansas, Department of Poultry Science) for her assistance with photography for this project. The authors also acknowledge the University of Arkansas Division of Agriculture for their support.

DISCLOSURES

There is no conflict of interest.

REFERENCES

- Abasht, B., M. F. Mutryn, R. D. Michalek, and W. R. Lee. 2016. Oxidative stress and metabolic perturbations in wooden breast disorder in chickens. *PLoS One* 11:e0153750.
- Baldi, G., F. Soglia, L. Laghi, S. Tappi, P. Rocculi, S. Tavaniello, D. Prioriello, R. Mucci, G. Maiorano, and M. Petracci. 2019. Comparison of quality traits among breast meat affected by current muscle abnormalities. *Food Res. Int.* 115:369–376.
- Barbin, D. F., S. M. Mastelini, S. Barbon, G. F. C. Campos, A. P. A. C. Barbon, and M. Shimokomaki. 2016. Digital image analysis as an alternative tool for chicken quality assessment. *Biosyst. Eng.* 144:85–93.
- Caldas-Cueva, J. P., A. Mauromoustakos, and C. M. Owens. 2021. Instrumental texture analysis of chicken patties prepared with broiler breast fillets exhibiting woody breast characteristics. *Poult. Sci.* 100:1239–1247.
- Caldas-Cueva, J. P., C. J. Maynard, A. Mauromoustakos, and C. M. Owens. 2020. Effect of woody breast condition on instrumental texture characteristics of poultry deli loaves. *Meat Muscle Biol.* 4:33, 1–10.
- Caldas-Cueva, J. P., and C. M. Owens. 2020. A review on the woody breast condition, detection methods, and product utilization in the contemporary poultry industry. *J. Anim. Sci.* 98:1–10.
- Chao, K., Y. R. Chen, W. R. Hruschka, and F. B. Gwozdz. 2002. Online inspection of poultry carcasses by a dual-camera system. *J. Food Eng.* 51:185–192.
- Chao, K., C. C. Yang, and M. S. Kim. 2010. Spectral line-scan imaging system for high-speed non-destructive wholesomeness inspection of broilers. *Trends Food Sci. Technol.* 21:129–137.
- Chatterjee, D., H. Zhuang, B. C. Bowker, A. M. Rincon, and G. Sanchez-Brambila. 2016. Instrumental texture characteristics of broiler pectoralis major with the wooden breast condition. *Poult. Sci.* 95:2449–2454.
- Dalgaard, L. B., M. K. Rasmussen, H. C. Bertram, J. A. Jensen, H. S. Møller, M. D. Aaslyng, E. K. Hejbøl, J. R. Pedersen, D. Elsser-Gravesen, and J. F. Young. 2018. Classification of wooden breast myopathy in chicken pectoralis major by a standardised method and association with conventional quality assessments. *Int. J. Food Sci. Technol.* 53:1744–1752.
- Geronimo, B. C., S. M. Mastelini, R. H. Carvalho, S. B. Júnior, D. F. Barbin, M. Shimokomaki, and E. I. Ida. 2019. Computer vision system and near-infrared spectroscopy for identification and classification of chicken with wooden breast, and physicochemical and technological characterization. *Infrared Phys. Technol.* 96:303–310.
- Hanning, C. O., X. Sun, J. P. Caldas-Cueva, and A. Mauromoustokos. 2020. System and Method for Detecting Woody Breast Condition in Broilers Using Image Analysis of Carcass Features (U.S. Patent No. 10,806,153). U.S. Patent and Trademark Office.
- Jiang, H., S. C. Yoon, H. Zhuang, W. Wang, K. C. Lawrence, and Y. Yang. 2018. Tenderness classification of fresh broiler breast fillets using visible and near-infrared hyperspectral imaging. *Meat Sci.* 139:82–90.
- Kuttappan, V. A., B. M. Hargis, and C. M. Owens. 2016. White striping and woody breast myopathies in the modern poultry industry: a review. *Poult. Sci.* 95:2724–2733.
- Martel, P., and D. Paris. 2007. Artificial Vision Inspection Method and System (U.S. Patent No. 20070111648). U.S. Patent and Trademark Office.
- Mehaffey, J. M., S. P. Pradhan, J. F. Meullenet, J. L. Emmert, S. R. McKee, and C. M. Owens. 2006. Meat quality evaluation of minimally aged broiler breast fillets from five commercial genetic strains. *Poult. Sci.* 85:902–908.
- Mollah, M. B. R., M. A. Hasan, M. A. Salam, and M. A. Ali. 2010. Digital image analysis to estimate the live weight of broiler. *Comput. Electron. Agric.* 72:48–52.
- Mudalal, S., M. Lorenzi, F. Soglia, C. Cavani, and M. Petracci. 2015. Implications of white striping and wooden breast abnormalities on quality traits of raw and marinated chicken meat. *Animal* 9:728–734.
- Park, B., and Y. R. Chen. 1994. Intensified multispectral imaging system for poultry carcass inspection. *Trans. ASAE.* 37:1983–1988.
- Petracci, M., F. Soglia, M. Madruga, L. Carvalho, E. Ida, and M. Estévez. 2019. Wooden-Breast, White Striping, and Spaghetti Meat: causes, consequences and consumer perception of emerging

- broiler meat abnormalities. *Compr. Rev. Food Sci. Food Saf.* 18:565–583.
- Russ, J. C. 2015. Image analysis of foods. *J. Food Sci.* 80:1974–1987.
- Sihvo, H. K., K. Immonen, and E. Puolanne. 2014. Myodegeneration with fibrosis and regeneration in the pectoralis major muscle of broilers. *Vet. Pathol.* 51:619–623.
- Soglia, F., J. Gao, M. Mazzoni, E. Puolanne, C. Cavani, M. Petracci, and P. Ertbjerg. 2017. Superficial and deep changes of histology, texture and particle size distribution in broiler wooden breast muscle during refrigerated storage. *Poult. Sci.* 96:3465–3472.
- Soglia, F., S. Mudalal, E. Babini, M. Di Nunzio, M. Mazzoni, F. Sirri, C. Cavani, and M. Petracci. 2016. Histology, composition, and quality traits of chicken pectoralis major muscle affected by wooden breast abnormality. *Poult. Sci.* 95:651–659.
- Sun, X., D. A. Koltjes, C. N. Coon, K. Chen, and C. M. Owens. 2018. Instrumental compression force and meat attribute changes in woody broiler breast fillets during short-term storage. *Poult. Sci.* 97:2600–2606.
- Tijare, V. V., F. L. Yang, V. A. Kuttappan, C. Z. Alvarado, C. N. Coon, and C. M. Owens. 2016. Meat quality of broiler breast fillets with white striping and woody breast muscle myopathies. *Poult. Sci.* 95:2167–2173.
- Velleman, S. G., D. L. Clark, and J. R. Tonniges. 2018. The effect of the wooden breast myopathy on sarcomere structure and organization. *Avian Dis.* 62:28–35.
- Wold, J. P., E. Veiseth-Kent, V. Høst, and A. Løvland. 2017. Rapid on-line detection and grading of wooden breast myopathy in chicken fillets by near-infrared spectroscopy. *PLoS One* 12:e0173384.
- Yoon, S. C., B. C. Bowker, and H. Zhuang. 2016. Toward a fusion of optical coherence tomography and hyperspectral imaging for poultry meat quality assessment. *IS and T International Symposium on Electronic Imaging. Image Processing: Machine Vision Applications IX*, pp. 1–5. Society for Imaging Science and Technology, Springfield, VA.
- Zambonelli, P., M. Zappaterra, F. Soglia, M. Petracci, F. Sirri, C. Cavani, and R. Davoli. 2016. Detection of differentially expressed genes in broiler pectoralis major muscle affected by White Striping – Wooden Breast myopathies. *Poult. Sci.* 95:2771–2785.